Journal of Chromatography A, 1219 (2012) 188–194

Contents lists available at SciVerse ScienceDirect

Journal of Chromatography A

journal homepage: www.elsevier.com/locate/chroma

# Characterization of cationic copolymers by capillary electrophoresis using indirect UV detection and contactless conductivity detection

Nadia Anik[a], Marc Airiau[b], Marie-Pierre Labeau[b], Chi-Thanh Vuong[b], Hervé Cottet[a,*]

[a] Institut des Biomolécules Max Mousseron, UMR CNRS 5247, Université de Montpellier 1, Université de Montpellier 2, CNRS, Place E. Bataillon, 34095 Montpellier, France
[b] Rhodia Opérations, Rue de la Haie Coq, 93308 Aubervilliers Cedex, France

ARTICLE INFO

*Article history:*
Received 26 August 2011
Received in revised form 6 November 2011
Accepted 8 November 2011
Available online 12 November 2011

*Keywords:*
Polyelectrolyte
Copolymers
Capillary electrophoresis
Capacitively coupled contactless conductimetry
Indirect UV detection

ABSTRACT

For many industrial applications, the combination of two different monomers in statistical or diblock copolymers enhances the properties of the corresponding polymer. However, during the polymerization reaction, homopolymers might be formed and can influence the properties for the applications. Consequently, the separation and the quantification of the homopolymers contained in copolymer samples are crucial. In addition, the charge density distribution of the statistical copolymer is an important characteristic for the applications. The purpose of this work was to study the characterization of a statistical copolymer of acrylic acid (AA) and diallyldimethyl ammonium chloride (DADMAC) by capillary electrophoresis (CE) in acidic conditions (cationic copolymers). For that purpose, a free solution electrophoretic separation was carried out according to the charge rate (chemical composition) independently of the molar mass. The second objective was to compare contactless conductivity detection and indirect UV absorbance modes for the quantification of DADMAC homopolymers present in copolymer samples. Different coated capillaries based on neutral or positively charged modification were also compared. The comparison of indirect absorbance UV and contactless conductimetric detection demonstrated that both detection modes can be used for a complete CE characterization of non-UV absorbing PAA-DADMAC copolymers.



## 1. Introduction

Copolymerization reactions provide an excellent way for the preparation of macromolecules with specific chemical compositions and structures which in turn allow to control properties such as solubility profile, viscosity profile, compatibility with complex formulations, affinity for surfaces and emulsifying properties. The characterization of these systems requires the use of a wide range of analytical tools (i) to control each step of synthesis, (ii) to determine the main physical and chemical characteristics and (iii) to study the organization in solution at molecular level. The main characteristics usually consist in the average molar mass, the dispersity, the chemical composition and its distribution, the content in residual monomers and homopolymers. Indeed, the presence of homopolymers in a copolymer sample can reduce the performances in the applications.

Among the separative techniques usually employed for polymer characterization, size exclusion chromatography (SEC) is the most popular one [1–3]. The deleterious effect of charges in SEC is notorious and the reproducibility (and thus accuracy) of SEC of polyelectrolytes is poor as exemplified for SEC of charged polysaccharides or the necessity to esterify copolymers of acrylic acid prior to SEC analysis [4]. Furthermore, separating homopolymers from copolymers by SEC requires differences in hydrodynamic volumes, a condition which is not always fulfilled. Capillary electrophoresis (CE) appears as a complementary tool to chromatography for polyelectrolyte characterization. CE presents the advantages to operate in an open medium without any stationary phase and to separate polyelectrolytes according to their charge density in free solution independently of the molar mass (so-called free draining behaviour [5,6]). In few words, the electric field pulls the chain in one direction and the counterions in the opposite one. This effect cancels the long-range hydrodynamic interactions between the monomers. Electric and hydrodynamic forces balance locally, which has two consequences: the electrophoretic mobility is independent of the size and the chain is not deformed in free solution electrophoretic conditions, even in a strong field [7].

Free solution CE has been reported to separate residual homopolymers from diblock copolymers. Jacquin et al. [8,9] quantified the proportion of poly (acrylic acid) (PAA) homopolymers in poly(butyl acrylate-b-acrylic acid) (PBA-b-PAA) copolymer samples. CE also allowed the monitoring of melting of kinetically

* Corresponding author. Tel.: +33 4 6714 3427; fax: +33 4 67 63 1046.
*E-mail address:* hcottet@univ-montp2.fr (H. Cottet).

0021-9673/$ – see front matter © 2011 Elsevier B.V. All rights reserved.
doi:10.1016/j.chroma.2011.11.014

frozen PBA-b-PAA micelles by the addition of small neutral surfactant [10]. Morel et al. [11] pointed out the presence of non micellized copolymers and polyelectrolyte homopolymers in associative dibloc poly(sodium vinyl acetate-co-acrylate) samples mainly composed of copolymer micelles. Homopolymers were also detected in copolymers samples by MEKC analysis [12] in the case of (2-hydroxyethyl methacrylate)-co-(2-acrylamido-2-methyl propane sulfonic acid) copolymers. For copolymer samples, free solution CE appears as a straightforward and simple characterization technique in comparison to liquid chromatography at the exclusion/adsorption transition (LC-PEAT) for which critical conditions relative to the polylelectrolyte block are difficult to implement and to reproduce.

Rhodia recently developed new statistical copolymers of acrylic acid (AA) and diallyldimethyl ammonium chloride (DADMAC) for home care applications. The main objective of this work was to characterize copolymer samples with different synthesis parameters. It was supposed to be especially relevant to quantify the proportion of remaining PDADMAC homopolymer in the copolymer samples. The main difficulties in this study stand in the non UV absorption of the PAA-DADMAC copolymer and PDADMAC homopolymer, as well as on polycation adsorption onto the capillary wall.

Polyelectrolytes that do not absorb in UV could be detected using indirect UV detection as exemplified on polyanions for glycosaminoglycanes (GAGs) [13–16], polysulfated pentosane [17], polyphosphates [18–20] or polycations [21,22]. Capacitively coupled contactless conductivity detection ($C^4D$) is an alternative detection mode of non UV absorbing polyelectrolytes. So far, there are very few examples in the literature on the use of $C^4D$ detection for polyelectrolyte or synthetic polymer analysis [23–25]. In this work, the two aforementioned detection modes were compared for the characterization of PAA-DADMAC copolymer samples.

## 2. Experimental

### 2.1. Chemicals

Sodium phosphate monobasic ($NaH_2PO_4$), imidazole was purchased from Aldrich (Steinheim, Germany). Creatinine, didodecyldimethylammonium bromide (DDAB) and poly(diallyldimethylammonium) chloride (PDADMAC, $M_w \sim 150{,}000$ g/mol) were purchased from Aldrich (Milwaukee, WI). Acetic acid was from Fluka (Seelze, Germany). Orthophosphoric acid (85%) was from Prolabo (Paris, France). Deionized water was further purified with a Milli-Q system from Millipore (Molsheim, France). Standard of poly(vinyl-4-pyridine) (PV4-p, $M_w$ 160,000 g/mol, dispersity of 1) was purchased from Polymer Standards Services (PSS, Germany).

### 2.2. Polymers

The PAADADMAC 60/40 mol/mol was prepared by radical polymerization in water phase. The AA was neutralized at pH = 6–7 before polymerization in order to improve the copolymerization with a less reactive monomer, DADMAC. The process used was a semi-continuous process under nitrogen with an initial charge of monomers (10%) at room temperature, following by the 4 h feedings of monomers (90%) and initiator, 2,2′-azobis(2-methylpropionamidine) dihydrochloride (1 mol%/monomers), at 70 °C.

### 2.3. Capillary electrophoresis

CE experiments were carried out with a $^{3D}$CE Agilent Technologies system (Waldbronn, Germany) equipped with a diode array detector. Separation capillaries prepared from bare silica tubing were purchased from Composite Metal Services (Worcester, UK). Capillary lengths were 33.5 cm (25 cm to the detector) × 50 μm for all analysis unless otherwise specified. New capillaries were conditioned by performing the following washes: 1 M NaOH for 20 min, 0.1 M NaOH for 15 min, and water for 10 min. The temperature of the capillary cassette was maintained constant at 25 °C. The polymer samples were prepared in deionized water. Sample volumes of approximately 4 nL were injected hydrodynamically (17 m bar, 5 s). The prepunchers and electrodes were cleaned each two days to remove solid deposits. Data were collected at 191, 192, or 207 nm depending on the electrolyte (see figure captions). Electroosmotic mobility was calculated from the migration time of mesityl oxide (neutral marker). Electropherograms were plotted in effective mobility scale ($\mu_{ep}$) using the following equation:

$$\mu_{ep} = \mu_{app} - \mu_{eo} = \frac{lL}{Vt_{app}} - \frac{lL}{Vt_{eo}} \quad (1)$$

where $l$ is the effective length up to the detection point, $L$ is the total capillary length, $V$ the applied voltage, $t_{app}$ the apparent detection time, and $t_{eo}$ the detection time of the neutral marker.

## 3. Theoretical background

### 3.1. Indirect UV detection (IUV)

IUV detection was first introduced in CE by Hjerten et al. [26]. In this detection mode, a UV absorbing co-ion, called the probe, is added to the background electrolyte (BGE). The indirect detection is due to the displacement of the probe by the solute leading to a decrease in the background absorbance. Therefore, a negative signal is recorded when the sample zone passes in front of the detector. The ability of the solute to displace the probe is directly related to the transfer ratio (TR), also called the displacement ratio or response factor, which is defined as the number of moles of displaced probe by mole of solutes. The signal response *Abs* in the sample zone is given by:

$$Abs = \varepsilon \times l \times \mathrm{TR} \times C_S \quad (2)$$

where $\varepsilon$ is the molar extinction coefficient of the probe at the detection wavelength, $l$ is the optical pathlength and $C_S$ is the molar concentration of the sample. It can be shown [27] that the change in concentration ($\Delta C_A$) in probe ion (A) caused by the solute (S) at concentration $C_S$ is given by the transfer ratio (TR):

$$\mathrm{TR} = \frac{|\Delta C_A|}{C_S^S} = \frac{z_S \mu_A (\mu_S + \mu_C)}{z_A \mu_S (\mu_A + \mu_C)} \quad (3)$$

where $z_A$ and $z_S$ are respectively the effective charges of the probe and solute. $\mu_A$, $\mu_S$ and $\mu_C$ are respectively the absolute values of effective mobilities of the probe, the solute and the counterion. Eq. (3) comes directly from the Kohlraush Regulating Function (KRF) [28] which is based on a balance of ion fluxes at the moving sample boundaries, and on the principle of electroneutrality, in absence of molecular diffusion. The KRF is a conservation law. It means that the KRF, also noted $w(x)$, is constant throughout the electrophoretic run at a given axial coordinate $x$ along the capillary following Eq. (4):

$$\sum \frac{z_i C_i}{\mu_i} = w(x) \quad (4)$$

where $C_i$, $z_i$ and $\mu_i$ represent ionic concentrations and absolute value of the charge and effective mobilities of all ionic constituents.

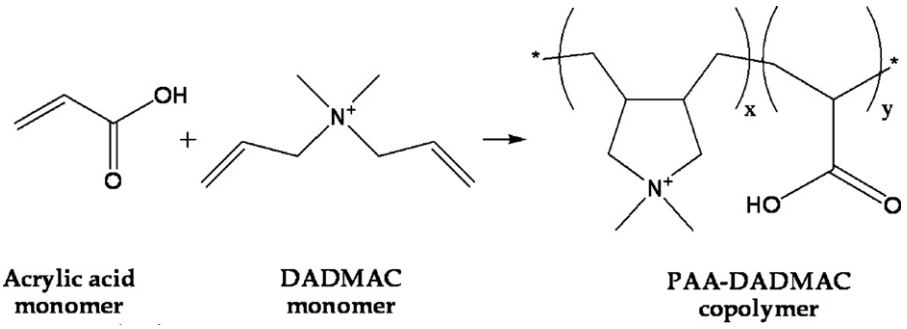


**Fig. 1.** Schematic representation of chemical structures of PAA-DADMAC copolymer and its monomers.

### 3.2. Capacitively coupled contactless conductimetric detection ($C^4D$)

$C^4D$ was introduced in CE in 1998 by Zeeman et al. [29] and Da Silva et al. [30]. In this detection mode, the detector is composed of two electrodes (or metallic rings) surrounding the capillary and distanced one each other of about 0.5 cm. The two rings are separated by a metallic sheet used as Faraday isolant to form two coupled capacitors. This system allows an easy and fast position control of the detector along the capillary, without removing the polyimide coating at the external surface of the capillary. The signal measured by the detector, namely the difference in conductance between sample zone (S) and background electrolyte (BGE), $\Delta G$, can be expressed as:

$$\Delta G = C_S \times \frac{(\mu_S - \mu_A)(\mu_S + \mu_C)}{\mu_S} \times \frac{F}{10^{-3}K} \quad (5)$$

where $\mu_A$, $\mu_C$ and $\mu_S$ are the absolute values of the effective mobility of co-ion, counter-ion and solute, respectively. $F$ is the Faraday constant and $K$ is the cellule constant. The optimization of the conductimetric signal consists in maximizing the $\Delta G$ function by changing the BGE constituents and mobilities. Nevertheless, this simplified equation only considers BGE with a single co-ion and counter-ion. For more complex BGE composition, it is possible to use the PeakMaster software based on a numerical modelling developed by Gas et al. [31–34]. This software (PeakMaster, http://www.natur.cuni.cz/~gas) calculates the intensity and the dispersion of the conductimetric signal. The main parameter, $b_S$ [35], defined by Eq. (6), allows an estimation of the $C^4D$ signal intensity relative to a solute $S$:

$$b_S = \lim_{C_{S\to 0}} \frac{d\kappa}{dC_S} \quad (6)$$

where $\kappa$ is the conductivity of the BGE and $d\kappa$ is the change in the conductivity at the point of detection, when the analyte zone with an infinitely small concentration $dC_S$ arrives into the detector cell. It is worth noting that the sign of $b_S$ indicates the polarity of the peak (positive value means positive solute peak, negative value indicates negative peak).

## 4. Results and discussion

Fig. 1 represents the chemical structures of acrylic acid (AA) and diallydimethylammonium chloride (DADMAC) monomers and the resulting PAA-DADMAC copolymer. The main objective of this work was to characterize different PAA-DADMAC copolymer for different synthesis conditions. Free solution CE was expected to bring information on the charge density distribution of the copolymer as well as on the proportion of residual PDADMAC homopolymer present in the samples. To reduce intra and inter-chains interactions, the copolymers were analyzed in acidic BGE to get a full protonation of the AA monomers. In these conditions, PAA-DADMAC copolymers are cationic polyelectrolytes. The chemical charge rate ($f$) of the copolymer is defined as the molar fraction of charged DADMAC monomer in the chain. $f$ was about 40% in average for all studied copolymer samples, as determined by NMR. However, no information on the charge density distribution was available.

To reduce polymer adsorption onto the capillary wall, two different approaches were compared: (i) neutral coating based on hydroxypropyl cellulose [36] or poly(vinyl alcohol) and (ii) a cationic double layer coating based on cationic double chain surfactant (didodecyldimethylammonium bromide, DDAB) [37,38]. It is worth noting that polyelectrolyte (or multi-polyelectrolyte layers) coatings cannot be used in this study because the electroosmotic mobility would be too low (in the range of $\sim 35–45 \times 10^{-5}$ cm$^2$ V$^{-1}$ s$^{-1}$) for the analysis of PDADMAC and PAA-DADMAC copolymers.

### 4.1. Optimization of the BGE for indirect UV detection

The choice of the probe for indirect UV detection depends on its electrophoretic mobility and on its molar extinction coefficient. Indeed, to avoid as much as possible peak asymmetry due to electromigration dispersion, the probe electrophoretic mobility should fit the solute mobility. PDADMAC homopolymer electrophoretic mobility is about $\sim 40 \times 10^{-5}$ cm$^2$ V$^{-1}$ s$^{-1}$, a typical value for a fully charged polyelectrolyte. PAA-DADMAC copolymers were expected to have slightly lower mobilities. Three cationic probes with different mobilities relatively close to solute mobilities were selected: imidazole (ionic mobility: $52 \times 10^{-5}$ cm$^2$ V$^{-1}$ s$^{-1}$), creatinine ($37 \times 10^{-5}$ cm$^2$ V$^{-1}$ s$^{-1}$) and poly(vinyl-4-pyridine) (Pv4-p, $\sim 40 \times 10^{-5}$ cm$^2$ V$^{-1}$ s$^{-1}$). Fig. 2 displays the electropherograms obtained for PDADMAC ($47 \times 10^3$ g/mol) sample (A) and for PAA-DADMAC copolymer (B) for the three aforementioned probes at a concentration of 6 mM in a phosphate buffer (pH 2.1) on a DDAB modified capillary. The detection wavelength was adjusted to the maximum of absorbance of each chromophore. For a better comparison, electropherograms were displayed in effective mobility scale. As shown in Fig. 2 and as calculated in Table 1, the sensitivities of detection $\alpha_S$ of PDADMAC and PAA-DADMAC increase in the order: imidazole < creatinine < Pv4-p. The sensitivity of detections $\alpha_S$ was determined using the slope of the calibration curve (time-corrected area of the solute vs its molar concentration). $\alpha_S$ values were in good agreement with Eq. (2) that states that the sensitivity of detection should increase linearly with $\varepsilon \times$ TR product (see $\varepsilon \times$ TR values in Table 1). Despite a higher sensitivity of detection for Pv4-p, creatinine was finally retained as the optimal probe because of better baseline stability and better resolution between PDADMAC and sodium. PDADMAC and PAA-DADMAC limits of detection (LOD at signal to noise ratio of 3) were experimentally determined in the creatinine-based BGE at 0.6 and 0.45 g/L, respectively.

**Table 1**
Comparison of different probes for PDADMAC and PAA-DADMAC detections in indirect UV mode.

| Probes | $\alpha_S$ (mAu L mol$^{-1}$) | | $\mu_A$ ($\times 10^{-5}$ cm$^2$ V$^{-1}$ s$^{-1}$) | $\mu_S$ ($\times 10^{-5}$ cm$^2$ V$^{-1}$ s$^{-1}$) | | $\mu_C$ ($\times 10^{-5}$ cm$^2$ V$^{-1}$ s$^{-1}$) | TR | | $\varepsilon$ Au L cm$^{-1}$ mol$^{-1}$ ($\lambda$ nm) | $\varepsilon \times$ TR (Au L cm$^{-1}$ mol$^{-1}$) | |
|---|---|---|---|---|---|---|---|---|---|---|---|
| | PDADMAC | PAA-DADMAC | | PDADMAC | PAA-DADMAC | | PDADMAC | PAA-DADMAC | | PDADMAC | PAA-DADMAC |
| Imidazole | 3.49 | 1.23 | 50.2 | 48.5 | 35.5 | 23.3 | 1.01 | 1.13 | 4303 (207) | 4346 | 4862 |
| Creatinine | 11.1 | 4.50 | 36.3 | 42.4 | 35.5 | 23.3 | 0.94 | 1.00 | 13666 (191) | 12846 | 13666 |
| Pv4-p | - | 5.51 | 39.65 | - | 37.5 | 23.3 | - | 1.02 | 11300 (192) | - | 11558 |

Electrophoretic conditions: Electrolyte for probe detection by direct UV detection: $H_3PO_4$ 12 mM, $NaH_2PO_4$ 6 mM, DDAB 0.1 mM. Electrolyte for PDADMAC ($47 \times 10^3$ g/mol) detection by IUV mode: 12 mM $H_3PO_4$, 6 mM probe, 0.1 mM DDAB, pH 2.1. Samples concentrations: 0.5–4 g/L. Applied voltage: −10 kV. Hydrodynamic injection: 17 m bar, 5 s. Temperature: 25 °C.




**Fig. 2.** Effective mobility scale electropherograms obtained for PDADMAC (A) and PAA-DADMAC copolymer (B) for three different probes. Electrophoretic conditions: fused silica capillary, 50 μm i.d. × 33.5 cm (effective length, 25 cm). Electrolyte: 12 mM $H_3PO_4$, 6 mM probe, 0.1 mM DDAB, pH 2.1. Applied voltage: −10 kV. Hydrodynamic injection: 17 m bar, 5 s. Indirect UV detection at 207 nm (imidazole), 191 nm (creatinine) and 192 nm (Pv4-p). Temperature: 25 °C. Samples: PDADMAC $47 \times 10^3$ g/mol at 1 g/L; PAA-DADMAC at 3 g/L. Peaks identification: PAA-DADMAC (1); PDADMAC (2); sodium (3); sodium and PDADMAC not fully separated (*).

### 4.2. Choice of the capillary coating

Fig. 3 represents the time-scale electropherograms obtained for a PAA-DADMAC copolymer in the previously optimized BGE (12 mM $H_3PO_4$, 6 mM creatinine and 0.1 mM DDAB) on a DDAB-modified fused silica capillary. This figure highlights the variations in EOF and the consequences on the separation of PDADMAC homopolymer, PAA-DADMAC copolymers and sodium ions. For strong EOF (trace A, EOF time: 1.77 min), PDADMAC (peak 2) is not fully separated from sodium ions (peak 3). For low EOF (trace C, EOF time: 2.3 min), longer migration times lead to peak broadening that strongly decreases the sensitivity of detection of PDADMAC. For intermediate EOF (trace B), separation is sufficient with reasonable dispersion, but the conditions are difficult to repeat and reproduce. Different procedures based on capillary flushes and rinsing were tried without any success.

To overcome this issue regarding the control of the EOF, a neutral hydroxypropylcellulose (HPC) coating was used. DDAB was removed from the BGE. In these conditions, the inner surface of the capillary is neutral and the EOF is very low. As shown

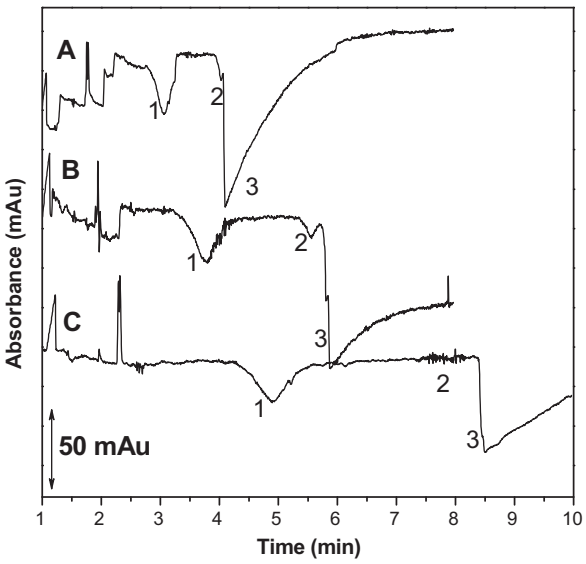


**Fig. 3.** Influence of EOF variations on the separation of PDADMAC homopolymer, PAA-DADMAC copolymer and sodium ions. Electrophoretic conditions: DDAB coated capillary, 50 μm i.d. × 33.5 cm (detector, 25 cm). Electrolyte: $H_3PO_4$ 12 mM, creatinine 6 mM, DDAB 0.1 mM (pH 2.5). Applied voltage: −10 kV. Hydrodynamic injection: 17 m bar, 5 s. Indirect UV detection at 191 nm. Temperature: 25 °C. Samples: PAA-DAMAC, 4 g/L. Peak identification: PAA-DADMAC (1); PDADMAC (2); $Na^+$ (3). EOF time: 1.77 min (A), 1.95 min (B), 2.3 min (C).

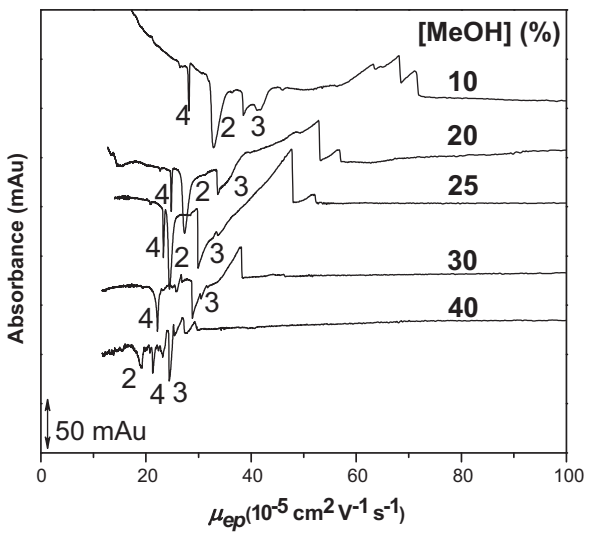


**Fig. 4.** Effective mobility-scale electropherograms displaying the separation of PDADMAC, DADMAC monomer and sodium ions for different methanol proportions in the electrolyte on a HPC coated capillary. Electrophoretic conditions: HPC coated capillary, 50 μm i.d. × 33.5 cm (detector, 25 cm). Electrolyte: 12 mM $H_3PO_4$, 6 mM creatinine in a water/methanol mixture as specified on the figure. Applied voltage: +10 kV. Hydrodynamic injection: 17 m bar, 5 s. Detection at 191 nm. Temperature: 25 °C. Samples: PDADMAC (47 × $10^3$ g/mol) 2 g/L; DADMAC monomer 0.1 g/L. Peak identification: PDADMAC (2); $Na^+$ (3); DADMAC monomer (4).

previously on the DDAB coated capillaries, the critical part concerns the separation of PDADMAC from sodium ions, due to the high peak dispersion and the large quantity of sodium in the sample. Interestingly, the addition of methanol in the BGE allows us to change and tune the selectivity between sodium ions, PDADMAC and DADMAC monomers as shown in Fig. 4 for different methanol concentrations ranging from 10 to 40% (v/v). When methanol concentration increases, PDADMAC mobility decreases faster than small ion mobilities. PDADMAC electrophoretic mobility becomes lower than DADMAC monomer mobility above 30% methanol in electrolyte. This faster decrease of mobility for polyelectrolyte is likely due to dielectric friction effect that increases considerably with the charge number of the solute and the concentration of organic solvent in the BGE [39,40]. It is worth noting that in Fig. 4, the injection time and the injection pressure were kept constant for all methanol concentrations. Since the viscosity of the electrolyte increases with the methanol proportion, the injected quantity decreases, as shown by the lower peak areas for higher methanol contents. A concentration of 25% in methanol brings a good compromise between separation time and resolution between sodium ion (peak 3, Fig. 4), PDADMAC (peak 2, Fig. 4) and DADMAC monomer (peak 4, Fig. 4).

Finally, optimal conditions for indirect UV detection of PDADMAC are: HPC coated capillary and BGE consisting in 12 mM $H_3PO_4$, and 6 mM creatinine in a 25% (v/v) MeOH/water mixture. In these conditions, the PDADMAC sensitivity of detection is slightly higher than that obtained on a DDAB coated capillary (15.6 vs 11.1 mAu L mol$^{-1}$). Furthermore, EOF is more stable and the dispersion of the PDADMAC peak is lower. The LOD of PDADMAC was substantially improved (about one order of magnitude) at 0.05 g/L. The RSD on the PDADMAC migration time was also much better on

**Table 2**
Electrolytes studied for the optimization of $C^4D$ detection.

| Electrolytes | | Co-ion 1 | Co-ion 2 | Counter-ion 1 | Counter-ion 2 | $b_x$ (mS m$^2$ mol$^{-1}$) | Electrolyte conductivity (S/m)[a] |
|---|---|---|---|---|---|---|---|
| 1. Acetic acid (1.15 M, | Ion | | $H^+$ | Acetate | | | |
| pH 2.3) | Mobility (×$10^{-9}$ m$^2$ V$^{-1}$ s$^{-1}$) | | 350 | −0.17 | | −11.1 | 0.18 |
| | Concentration (mM) | | 1145 | 4.87 | | | |
| 2. Acetic acid | Ion | | $H^+$ | Acetate | $Cl^-$ | | |
| (1.15 M) + HCl (1 mM) | Mobility (×$10^{-9}$ m$^2$ V$^{-1}$ s$^{-1}$) | | 350 | −0.15 | −75.4 | −14.1 | 0.21 |
| (pH 2.3) | Concentration (mM) | | 1146 | 4.4 | 1 | | |
| 3. Acetic acid | Ion | | $H^+$ | Acetate | $Cl^-$ | | |
| (1.15 M) + HCl (3 mM) | Mobility (×$10^{-9}$ m$^2$ V$^{-1}$ s$^{-1}$) | | 350 | −0.12 | −75.2 | −21.4 | 0.26 |
| (pH 2.2) | Concentration (mM) | | 1146 | 3.6 | 3 | | |
| 4. Acetic acid | Ion | | $H^+$ | Acetate | $Cl^-$ | | |
| (1.15 M) + HCl (5 mM) | Mobility (×$10^{-9}$ m$^2$ V$^{-1}$ s$^{-1}$) | | 350 | −0.1 | −75 | −29.3 | 0.32 |
| (pH 2.1) | Concentration (mM) | | 1147 | 3 | 5 | | |
| 5. β-Alanine | Ion | $H^+$ | β-alanine$^+$ | β-Alanine$^-$ | $Cl^-$ | | |
| (10 mM) + HCl (20 mM) | Mobility (×$10^{-9}$ m$^2$ V$^{-1}$ s$^{-1}$) | 350 | 33.12 | ∼0 | −73.2 | 17.6 | 0.52 |
| (pH 2) | Concentration (mM) | 20 | 9.65 | ∼0 | 20 | | |
| 6. Histidine | Ion | $H^+$ | Histidine$^+$ | Histidine$^-$ | $Cl^-$ | | |
| (10 mM) + HCl (20 mM) | Mobility (×$10^{-9}$ m$^2$ V$^{-1}$ s$^{-1}$) | 350 | 28.83 | ∼0 | −72 | 12.8 | 0.37 |
| (pH 2.3) | Concentration (mM) | 20 | 5.72 | ∼0 | 20 | | |

[a] Determined by PeakMaster software.

the HPC coated capillary (2%, $n = 5$ injections) than with the DDAB coated capillary (12%, $n = 5$ injections). It is worth noting that similar results could be obtained with a PVA coated capillary instead of the HPC capillary.

### 4.3. Optimization of the BGE for $C^4D$ detection

Optimizing the BGE for $C^4D$ detection requires to maximize the detector response $\Delta G$ given by Eq. (5) (or $b_x$ given by PeakMaster software, in the case of multi-components BGE) while keeping a reasonable peak dispersion and a reasonable overall conductivity. Eq. (5) states that the detector response should increase when the counter-ion mobility increases (in absolute value) and when the difference in mobility between the solute and the co-ion increases. Nevertheless, large differences between solute and co-ion mobilities tend to increase the peak dispersion by electromigration. Therefore, there is a compromise between the peak dispersion and the sensitivity of the detection. Starting with a conventional acetic acid-based BGE (pH 2.5), that has been widely used for $C^4D$ detection in acidic conditions [41,42], some HCl was added (from 1 to 5 mM) in the BGE to increase the mobility of the counter-ion, and thus the sensitivity of detection. As expected, the $b_x$ values given by PeakMaster increase with the addition of HCl (see Table 2 for the composition of the different tested BGE and the corresponding $b_x$ values). The increase in sensitivity by addition of HCl was also accompanied with peak dispersion and some loss in resolution between PDADMAC and monomer DADMAC signal (not shown). At 5 mM HCl, baseline instability was observed. The optimal compromise between sensitivity of detection and resolution was obtained with the BGE containing 1 mM HCl and 1.15 M acetic acid. Two other BGE based on β-alanine/HCl and histidine/HCl were also tried without success, while $b_x$ values were similar in absolute value to that of the optimal acetic acid/1 mM HCl BGE. As for acetic acid BGE containing 5 mM HCl, the conductivity was likely too high (see Table 2 for values) and instability baseline was observed.

### 4.4. Comparison between $C^4D$ and IUV detection modes

The two aforementioned and optimized detection modes were finally compared in terms of sensitivity of detection and LOD for the analysis of PDADMAC and PAA-DADMAC copolymer. Table 3 presents the figures of merits in the optimal conditions. Regarding the PDADMAC, the sensitivity of detection is slightly higher than for the copolymer, whatever the detection mode. This can be easily explained since the effective charge of the PDADMAC is higher than that of the PAA-DADMAC which increases the IUV sensitivity of detection. In the case of the $C^4D$ detection mode, the higher sensitivity for the PDADMAC can be explained by its higher mobility than that of the copolymer. On the whole, better LODs were obtained using $C^4D$ than IUV detection by a factor of 5–20. LODs of the PDADMAC and PAA-DADMAC using optimal BGE conditions and $C^4D$ detection were both about 0.01 g/L. Nevertheless, for the quantification of residual PDADMAC homopolymer in the copolymer sample, IUV detection was found to be more robust in terms of baseline stability. Despite a higher LOD compared to $C^4D$, PDADMAC quantification was found to be more convenient using IUV detection with less interference due to a different order of detection relative to sodium ion.

### 4.5. Characterization of PAA-DADMAC copolymer samples having different synthesis parameters

Three PAADAMAC copolymer samples of which present different synthesis parameters (A, B, C) were analyzed in the previously described optimal conditions. Fig. 5 represents mobility-scale electropherograms obtained for copolymers A, B and C by IUV detection

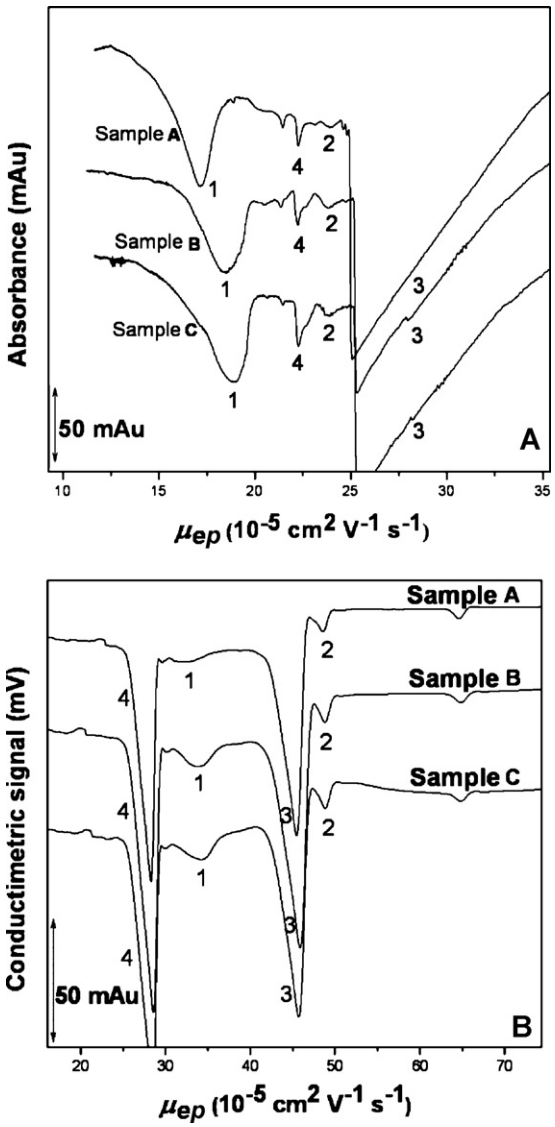


**Fig. 5.** Characterization of three different PAA-DADMAC copolymer samples by IUV (A) and $C^4D$ (B) detection modes. Electrophoretic conditions: (A) HPC coated capillary, 50 μm i.d. × 33.5 cm (detector, 25 cm). Electrolyte: $H_3PO_4$ 12 mM, creatinine 6 mM in a water/methanol (75/25, v/v) mix media. Applied voltage: +10 kV. Hydrodynamic injection: 17 m bar, 5 s. Indirect UV detection at 191 nm. Temperature = 25 °C. Samples: PAA-DAMAC A, B, C at 16 g/L + DADMAC monomer 0.05 g/L. Peak identification: PAA-DADMAC (1); PDADMAC (2); $Na^+$ (3); DADMAC monomer (4). (B) PVA coated capillary, 50 μm i.d. × 33.5 cm (detector, 21 cm). Electrolyte: 1.15 M acetic acid + 1 mM HCl. Applied voltage: +10 kV. Hydrodynamic injection: 17 m bar, 5 s. Temperature = 25 °C. Samples: PAA-DAMAC A, B and C at 0.5 g/L + DADMAC monomer 0.5 g/L. Peak identification: Peak identification: PAADADMAC (1); PDADMAC (2); $Na^+$ (3); DADMAC monomer (4).

(Fig. 5A) and $C^4D$ detection (Fig. 5B). Both modes of detection allowed to distinguish the average effective mobility of copolymer A from the others. Copolymer A presented a lower average mobility value than that observed for the others (see Table 4 for the numerical values). The differences in the average mobility values observed with the two detection modes is too high to be explained by the differences in ionic strength between the two BGE. Specific interaction between PDADMAC and/or the copolymer with phosphate ions could be at the origin of the lower mobility observed in the phosphate based BGE. No significant difference of effective mobility could be determined between copolymer B and C. This can be concluded by comparing the difference between the average effective mobility values relatively to the peak dispersion that was estimated

**Table 3**
Comparison of the sensitivities of detection and the LOD obtained by IUV and $C^4D$ for PDADMAC and PAA-DADMAC.

| Capillary coating/detection mode | PDADMAC | | | | PAA-DADMAC | | | |
|---|---|---|---|---|---|---|---|---|
| | Detection sensitivity ($mV\,L\,mol^{-1}$) | Noise (mV) | LOD (g/L) | RSD on $t_m$ ($n=5$)[a] | Detection sensitivity ($mV\,L\,mol^{-1}$) | Noise (mV) | LOD (g/L) | RSD on $t_m$ ($n=5$)[a] |
| HPC/IUV | 15.6 | 1 | 0.05 | 2 | 4.8 | 0.37 | 0.23 | 2.6 |
| PVA/$C^4D$ | 31.2 | 0.15 | 0.01 | 3.7 | 10.5 | 0.11 | 0.01 | 6.4 |

Electrophoretic conditions, IUV: HPC coated capillary, 50 μm i.d. × 33.5 cm (detector, 25 cm). Electrolyte: 12 mM $H_3PO_4$, 6 mM creatinine in a (75/25, v/v) water/methanol mixture. Electrophoretic conditions, $C^4D$: PVA coated capillary, 50 μm i.d. × 33.5 cm (detector, 25 cm). Electrolyte: 1.15 M acetic acid, 1 mM HCl. Other conditions: Applied voltage: +10 kV. Hydrodynamic injection: 17 m bar, 5 s. Temperature: 25 °C.

[a] RSD on migration time of PAA-DADMAC copolymer in %.

**Table 4**
Average effective mobility, standard deviation on the mobility distribution and mass proportion of residual PDADMAC for different PAA-DADMAC copolymer samples.

| Copolymers | % PDADMAC in copolymer sample | IUV detection | | $C^4D$ detection | |
|---|---|---|---|---|---|
| | | $\mu$ ($\times10^{-5}$ $cm^2\,V^{-1}\,s^{-1}$) | $\sigma_\mu$ ($\times10^{-5}$ $cm^2\,V^{-1}\,s^{-1}$) | $\mu$ ($\times10^{-5}$ $cm^2\,V^{-1}\,s^{-1}$) | $\sigma_\mu$ ($\times10^{-5}$ $cm^2\,V^{-1}\,s^{-1}$) |
| A | 0.3 | 15.84 | 1.34 | 38.94 | 1.49 |
| B | 1.1 | 18.73 | 0.79 | 40.67 | 1.20 |
| C | 0.7 | 18.22 | 1.01 | 40.38 | 1.91 |

Electrophoretic conditions: see Fig. 5.

by the standard deviation on the effective mobility distribution $\sigma_\mu$ (see Table 4). The weight proportion of PDADMAC in the copolymer samples was about 0.3–1.1%, as calculated from a calibration curve using PDADMAC ($47 \times 10^3$ g/mol) standard solutions.

## 5. Conclusion

The comparison of indirect absorbance UV and contactless conductimetric detection demonstrated that both detection modes can be used for a complete CE characterization of non-UV absorbing PAA-DADMAC copolymer samples (charge density distribution and homopolymer or monomer contents). Different coated capillaries based on neutral (HPC, PVA) or positively charged modification (DDAB) were also studied and compared. Neutral coated capillary (HPC) gave the best results in terms of repeatability and baseline stability/noise compared to DDAB coated capillary. $C^4D$ detection led to the best LODs about 0.01 g/L for both PDADMAC homopolymer and PAA-DADMAC copolymer (40% mol in charged monomer). In the optimal conditions, repeatability on migration time was 2% and the separation was realised in less than 10 min. Regarding the differences between the three real copolymer samples, capillary electrophoresis pointed out a difference in the average effective mobility of copolymer A from the other samples. No significant difference in the dispersion of the charge rate distribution between the three samples was observed. Finally, the proportion of residual PDADMAC homopolymers (from 0.3% to 1.1%) could be reliably measured, which makes capillary electrophoresis a powerful tool for optimization of synthesis parameters.

## References

[1] H. Pasch, B. Trathnigg, HPLC of Polymers, Springer, Heidelberg, Germany, 1997.
[2] M. Fontanille, Y. Gnanou, Chimie et Physico-chimie des Polymères, Dunod, Paris, 2002.
[3] Y. Guillaneuf, P. Castignolles, J. Polym. Sci. Part A: Polym. Chem. 46 (2008) 897.
[4] G. Delaittre, B. Charleux, Macromolecules 41 (2008) 2361.
[5] H. Cottet, C. Simó, W. Vayaboury, A. Cifuentes, J. Chromatogr. A 1068 (2005) 59.
[6] H. Cottet, G. Gareil, in: P. Schmitt-Kopplin (Ed.), CE from Small Ions to Macromolecules, Humana Press, Totowa, NJ, 2008, p. 541.
[7] D. Long, J.L. Viovy, A. Ajdari, J. Phys. Condens. Matter 8 (1996) 9471.
[8] M. Jacquin, P. Muller, R. Talingting-Pabalan, H. Cottet, J.F. Berret, T. Futterer, O. Théodoly, J. Colloid Interface Sci. 316 (2007) 897.
[9] M. Jacquin, P. Muller, G. Lizaraga, C. Bauer, H. Cottet, O. Théodoly, Macromolecules 40 (2007) 2672.
[10] M. Jacquin, P. Muller, H. Cottet, R. Crooks, O. Théodoly, Langmuir 23 (2007) 9939.
[11] A. Morel, H. Cottet, M. In, S. Deroo, M. Destarac, Macromolecules 38 (2005) 6620.
[12] M.R. Aguilar, A. Gallardo, J. SanRoman, A. Cifuentes, Macromolecules 35 (2002) 8315.
[13] J. Grimshaw, Electrophoresis 18 (1997) 2408.
[14] W. Mao, C. Thanawiroon, R.J. Linhardt, Biomed. Chromatogr. 16 (2002) 77.
[15] M.Y. Kim, A. Varenne, R. Daniel, P. Gareil, J. Sep. Sci. 26 (2003) 1154.
[16] M. Degenhardt, H. Benend, H. Wätzig, J. Chromatogr. A 817 (1998) 297.
[17] S. Prochazka, M. Mulholland, A. Lloyd-Jones, J. Pharm. Biomed. Anal. 31 (2003) 133.
[18] T. Wang, S.F.Y. Li, J. Chromatogr. A 723 (1996) 197.
[19] T. Wang, S.F.Y. Li, J. Chromatogr. A 802 (1998) 159.
[20] A. Lee, G.M. Whitesides, Anal. Chem. 82 (2010) 6838.
[21] H. Engelhardt, M. Martin, Adv. Polym. Sci. 165 (2004) 211–247.
[22] O. Grosche, J. Bohrisch, U. Wendler, W. Jaeger, H. Engelhardt, J. Chromatogr. A 894 (2000) 105.
[23] K.A. Oudhoff, M. Macka, P.R. Haddad, P.J. Schoenmakers, W.T. Kok, J. Chromatogr. A 1068 (2005) 183.
[24] K.H. Spriestersbach, F. Rittig, H. Pasch, Electrophoresis 29 (2008) 4407.
[25] P. Tůma, E. Samcová, F. Opekar, K. Štulík, Collect. Czech. Chem. Commun. 73 (2) (2008) 187.
[26] S. Hjerten, K. Elenbring, F. Kilar, J. Liao, A.J.C. Chen, C.J. Siebert, M. Zhu, J. Chromatogr. 403 (1987) 47.
[27] C. Johns, M. Macka, P.R. Haddad, Electrophoresis 24 (2003) 2150.
[28] F. Kohlraush, Ann. Phys. 62 (1897) 209.
[29] A.J. Zemann, E. Schnell, D. Volgger, G.K. Bonn, Anal. Chem. 70 (1998) 563.
[30] J.A. Fracassi da Silva, C.L. Do Lago, Anal. Chem. 70 (1998) 4339.
[31] M. Jaros, K. Vcelakova, I. Zuskova, B. Gas, Electrophoresis 23 (2002) 2667.
[32] M. Jaros, V. Hruska, M. Stedry, I. Zuskova, B. Gas, Electrophoresis 25 (2004) 3080.
[33] M. Jaros, T. Soga, T. Van de Goor, B. Gas, Electrophoresis 26 (2005) 1948.
[34] B. Gas, P. Coufal, M. Jaros, J. Muzikar, I. Jelinek, J. Chromatogr. A 905 (2001) 269.
[35] P. Gebauer, J. Caslavska, W. Thormann, P. Bocok, J. Chromatogr. A 772 (1997) 63.
[36] Y. Shen, R.D. Smith, J. Microcolumn Sep. 12 (2000) 135.
[37] J.E. Melanson, C.A. Lucy, J. Chromatogr. A 884 (2000) 311.
[38] J.E. Melanson, N.E. Baryla, C.A. Lucy, Anal. Chem. 72 (2000) 4110.
[39] J. Hubbard, L. Onsager, J. Chem. Phys. 67 (1977) 4850.
[40] K.I. Roy, C.A. Lucy, Electrophoresis 24 (2003) 370.
[41] P. Coufal, J. Zuska, T. Van de Goor, V. Smith, B. Gas, Electrophoresis 24 (2003) 671.
[42] S. Anouti, O. Vandenabeele-Trambouze, H. Cottet, Electrophoresis 31 (2010) 1029.